63-2-3

Second Quarterly Progress Report

30 June to 30 September 1962

SOLID STATE S- AND X-BAND LIMITERS

Contract NObsr - 87307

Project Serial No. SR0080301, ST9386

Placed by:

Navy Department Bureau of Ships

MICROWAVE ASSOCIATES, INC.
BURLINGTON, MASSACHUSETTS

MICROWAVE ASSOCIATES, INC.

Second Quarterly Progress Report

30 June to 30 September 1962

SOLID STATE S- AND X-BAND LIMITERS

Contract NObsr - 87307

Project Serial No. SR 0080301, ST 9386

Navy Department Bureau of Ships

Prepared by:

Robert Tenenholtz

Approved by:

Dr. Kenneth E. Mortenson

MICROWAVE ASSOCIATES, INC.

Burlington, Massachusetts

TABLE OF CONTENTS

ABSTRACT

During the second quarterly period of this report, efforts in X-band were continued. In addition, work in the S- region was initiated. An analysis of several modes of limiter operation is made and a comparison of theoretical performance is performed. Experimental data for both X- and S-bands is presented showing present capabilities to be 500 and 1000 watts peak respectively. This does not assume paralleling units which would result in a 3 DB increase.

Types of diodes used are mentioned along with their general operational characteristics. Spike leakage associated with high power type diodes used is described along with general measured characteristics for both frequency regions of operation.

PART I

PURPOSE

The purpose of work conducted under this program is to investigate methods leading to the design of solid state microwave limiters employing PN junctions at S-and X-band. Tentative design goal specifications are as follows:

	S-Band	X-Band
Peak Power, min.	10	1.0 KW
Avg. Power, min.	10	1.0 W
Insertion Loss, max.	1.0	1.0 DB
Isolation, min.	40	30 DB
Bandwidth, min.	10	7.5 %

In addition, techniques capable of extending operation to even higher power levels will also be reviewed.

GENERAL FACTUAL DATA

A. INTRODUCTION

In the previous quarterly report, an initial analysis was made with respect to X-band operation of a PN-junction limiter. This effort has been continued in order to secure optimum limiter design information and has also been extended down to S-band. Methods of analysis, equivalent circuits and theoretical results are presented in the following sections.

1. The Shunt Transmission PN-Junction Limiter

The shunt transmission PN-junction limiter mode of operation can be considered as an equivalent power sensitive attenuator. At low power levels, little attenuation is encountered. However, as incident power increases, effective attenuation of the device becomes larger with a resultant limiting action taking place. Two circuits capable of performing this function are shown in Figure (1). These will be termed shunt transmission modes I and II.

In both limiter modes, limiting is secured by interaction of applied power on C_s and R_s. These values represent PN-junction series capacitance and resistance respectively as would be evident under low power conditions. In the case of high incident power applied, a drastic change occurs and the new values of $\bar{C}_s$ and $\bar{R}_s$ are present. For all practical purposes $\bar{C}_s$ can be considered infinite and its impedance value neglected. As for $\bar{R}_s$, it will be less than R_s due to conductivity modulation. Past work in this area has shown the relationship $\bar{R}_s = .2R_s$ to be a good approximation of the actual values encountered.

In mode I, the value θ_1 is so adjusted such that a minimum value shunting impedance appears across the the transmission line $\mathcal{Z}_o$ when high power is

encountered. This will appear as a virtual short circuit and result in high isolation between terminal pairs 1 and 2. Once θ is determined, X_E is adjusted to resonate any shunting reactance across $\mathcal{Z}_o$ under low power conditions.

In mode II, a similar procedure is used to determine both θ_2 and X_E. However, in this case, the varactor is used to terminate the auxilliary arm $\mathcal{Z}_o'$ where as it was placed in series in the preceding example.

In order to evaluate either of these modes, it would be convenient to first secure a series impedance representation of the varactor. This can be accomplished by use of the following equations:

$$R_T = \frac{X_p^2 R_s}{R_s^2 + (X_s + X_p)^2} \qquad (1)$$

$$X_T = \frac{X_p R_s^2 + (X_s + X_p) X_s X_p}{R_s^2 + (X_s + X_p)^2} \qquad (2)$$

where R_T and X_T are the equivalent PN-junction diode series impedance components

X_s is the sum reactance due to C_s and L_s

X_p is the reactance due to C_p

R_s is the PN-junction series resistance

The values $\overline{R_T}$ and $\overline{X_T}$ * may now be employed in appropriate relationships to secure the various necessary values of θ. For mode I operation this can be expressed as

$$\theta_1 = \tan^{-1} - \frac{\overline{X_T}}{\mathcal{Z}_o'} \qquad (3)$$

---

* Bar designation denotes high power impedance values.

This is arrived at by equating the impedance sum of $\bar{X}_T$ and a shorted line length of $\bar{z}_o'$ to zero. From this, the line length θ_1 can be solved for as shown in the above equation.

In the case of mode II, the line length θ_2, can be solved for by setting up the equation of a transmission line, $\bar{z}_o'$, terminated by the varactor under high power conditions. To a first approximation the effect of $\bar{R}_s$ may be neglected and the varactor package treated as a pure reactance. Using this approach, the expression for θ_2 becomes identical to that for θ_1 in equation (3).

With required values of θ determined along with specific PN-junction diode characteristics, the equivalent normalized shunt admittance components appearing across the main transmission line, $\bar{z}_o$, can be computed. These will be expressed as $g + jb$ and $\bar{g} + j\bar{b}$ for low and high power conditions respectively. Once available, loss equations as given in Figure (2) may be used to determine limiter loss characteristics.

2. The Shunt Reflection PN-Junction Limiter

In addition to the transmission modes of operation previously described there exists the possibility of a reflection type mode. Whereas the former could be compared to a TR type duplexer, the latter could be characterized by an ATR configuration. This implys that a reflective type PN-junction limiter would appear highly reflective under low power conditions and appear as a matched device when subjected to high power levels. Therefore, some auxiliary such as a hybrid or ferrite circulator would also be required.

As for now only the PN-junction limiter circuit itself will be considered for initial evaluation. A circuit capable of performing the desired action as mentioned above is shown in Figure (3). This appears to be very similar

to the mode I shunt transmission type as illustrated in Figure (1). However, in this case, an additional shunting capacitance, C_x, is added across the PN-junction diode terminals. Its purpose is to resonate the parallel combination of C_p and L_x under high power conditions. The reactance contribution of $\bar{C}_s$ is again neglected due to its very low value under high power conditions. Therefore, a very large impedance will appear across the main transmission line, $\bar{z}_o$, under high power conditions.

Under low power conditions, the line length, θ_3, is so chosen as to series resonate with the parallel combination of the PN-junction diode and C_x. This will then effectively place a short circuited condition across the main transmission line and result in any incoming signal being reflected. By utilizing this circuit with a ferrite circulator on the input side and a matched termination on the output, desired limiting action can be secured.

In order to determine the value of θ_3 required, an analysis similar to that presented for the cases may be employed. However, here, the presence of C_x must be accounted for. This can be accomplished by assuming the parallel combination of C_p and C_x to be a new PN-junction diode shunting capacitance. Therefore the value X_p as used in equations (1) and (2) must be modified to account for the effect of C_x. This will result in new values for the PN-junction diode series equivalent circuit impedance components. These will be differentiated from the previous values by the notation R_{Tx} and X_{Tx}. Therefore, θ_3 may be determined by use of the following equation

$$\theta_3 = \tan^{-1} - \frac{X_{Tx}}{\bar{z}_o'} \qquad (4)$$

With θ_3 known, equivalent normalized shunt admittance components appearing across $\bar{z}_o$ can be computed. By use of these values in loss equations

presented in Figure (4), initial limiter performance characteristics may be determined.

3. Theoretical Comparison of Transmission and Reflection Limiter Mode Performance

In order to secure some form of operational comparison of the various limiter modes described, a varactor of specific characteristics will be assumed utilized in each case of interest. Once R_T and X_T are computed, θ values are determined. The impedance shunting the main transmission line z_o can then be calculated. This will be represented by the values R_T' and X_T' where the prime notation denotes impedance of the varactor as modified by the transmission line z_o'. In order to utilize loss equations presented in Figures (2) and (3) $R_T'+jX_T'$ must be converted into a set of normalized admittance components. This is accomplished by use of equations (5) and (6) as given below:

$$g = \frac{z_o R_T}{\left(R_T'\right)^2 + \left(X_T'\right)^2} \qquad (5)$$

$$b = \frac{z_o X_T'}{\left(R_T'\right)^2 + \left(X_T'\right)^2} \qquad (6)$$

Using the previously described procedures for determining insertion loss and isolation*, a varactor of specific characteristics can be used to determine comparative performance of the limiters previously described. Results of this are shown in Table (1).

---

* Isolation refers to high power loss exhibited by the limiter.

TABLE I

THEORETICAL COMPARATIVE PERFORMANCE OF

SEVERAL VARACTOR LIMITER TYPES

VARACTOR CHARACTERISTICS

C_o	0.8 $\mu\mu$f
f_{co}	60 KMc
L_s	2 mμh
C_p	0.4 $\mu\mu$f

LIMITER CIRCUIT CHARACTERISTICS

$\bar{z}_o = \bar{z}_o' = 50\ \Omega$

FREQUENCY OF OPERATION

3.0 KMc

CHARACTERISTIC	SHUNT TRANS. MODE I	SHUNT TRANS. MODE 2	SHUNT REF. MODE 3
g	.0194	.0483	46.8
$\bar{g}$	38.8	100	.0232
IL, DB	0.07	0.2	0.3
$\overline{IL}$, DB	25.7	34.	38.8
% Power Dissipated In $\bar{R}_s$	9.4	3.85	2.25

In Table I, in addition to characteristics previously described, percent power dissipated in $\bar{R}_s$ is also listed. This can be secured from the general expression of equation (7)

$$\% \text{ Power Diss} = \frac{400\, g}{g^2 + 4g + 4} \qquad (7)$$

Inspection of Table I shows the reflection mode to yield best high power performance with power dissipated by the varactor used as the criteria. For best low level performance, shunt transmission mode I is superior on the basis of insertion loss and mode 2 exhibits a compromise between the two extremes. Therefore, as for which one to use in a particular application, a varity of choices exist and a choice can be made on the basis of most pertinent operational characteristics desired.

Before concluding this section, it must be remembered that though the shunt reflection mode offers best high power limiter characteristics, it suffers not only from higher insertion loss but also circuit complexity. This arises from the fact that some auxiliary devices must also be employed, such as loads, circulators, hybrids, etc.

IDENTIFICATION OF PERSONNEL

		Man Hours
K. Mortenson	Director of R & D -- Physicist	32
R. Tenenholtz	Group Leader -- Circuit Engineer	53
C. Howell	Group Leader -- Semiconductor Engineer	86
H. Mooncai	Circuit Engineer	125

DETAILED FACTUAL DATA

A. Introduction

Previous to the period covered by this report, all experimental work of any significance had been devoted to the area of X-band operation. Since then work has been initiated at S-band and efforts in X-band continued to a point where 500 watt peak power operation has been successfully achieved. Details of this are described in the following sections.

1. S-Band Experimental Results

Initial work in S-band has taken the form of investigating various coaxial structure configurations. These are shown in Figure (5). Placement of the limiter diodes is in accordance with equivalent circuit schematics as shown in Figures (1) and (3). Coaxial connectors utilized were type N and have been eliminated from Figure (5) for the sake of simplicity. In both cases, the 450 type package was used. For the shunt reflection mode of operation, insulated aluminum tape was wrapped around the ceramic portion of the 450 package to provide the external tuning capacitance, C_x, necessary for proper operation.

In Figure (6) performance characteristics are shown for a shunt transmission mode 2 limiter. The top illustration shows a plot of zero bias insertion loss versus frequency. Also presented is a plot of simulated isolation which is achieved by application of a forward bias current of +25 ma. For this particular case, the low level tuning reactance X_E as shown in Figure (1) was found to be unnecessary and omitted. Its inclusion would have possibly resulted in improving insertion loss by only a small fraction of a DB.

The diode used for this particular case was a 500V PIN type. This is very similar to a varactor except that a relatively large intrinsic region is placed between the P^+ and N^+ regions. This technique enables extremely high values of reverse voltage breakdown to be secured and thus greater power handling

capability. However, the price paid is relatively sluggish operation with a somewhat pronounced spike occurring similar to that found in gas TR tubes. To minimize this, a crystal is used to sample incoming power and its rectified output fed into the PIN diode. The crystal itself has a sub-nanosecond speed of response.

The lower portion of Figure (6) illustrates high power performance over the frequency range of interest. Isolation never exceeds 12 DB because of the spike which was found to have an equivalent rectangular pulse width of 0.13μs. The applied high power signal had a 1.0μs pulse width and pulse rep. rate of 1000 cps. At 2.9 KMc, the peak spike value was measured and found to be 575 watts with an accompanying flat level of 60 watts.

In Figure (7), first initial results on securing a successful reflection mode form of operation are presented. For this particular test a varactor was used and its characteristics are listed in Figure (7) also. Insertion loss figure shown were computed from VSWR measurements under low applied power conditions. A lossless circulator was assumed. Simulation of high power isolation was achieved by application of a +25 ma bias current. The value of isolation secured was calculated from measured VSWR with the limiter terminated by a matched load.

High power tests were run at 3.0 KMc with a 1.0μs pulse width and 1000 cps. rep. rate. At peak power level of 800 watts, an isolation value of 9.1 DB was secured. In this case, no spike was present as would be anticipated since a varactor was used. The capacitance C_x, necessary for proper operation was secured by wrapping aluminum tape around the ceramic portion of the diode package.

2. X-Band Experimental Results

In the last quarterly report, preliminary X-band results were reported on

the configuration shown in the top illustration of Figure (8). For this particular situation a pill type package was used rather than the 450 due to lower parasitic reactance values. This is effectively a shunt transmission mode 2 form of operation with Z_o in waveguide and Z'_o being coax. However, it does differ in one respect which is that a shunt capacitance is placed across the varactor package as in the reflection mode form of operation. This shunt capacitance is achieved by inserting the diode partially into the coaxial choke. The capacitance value must be sufficiently large to create a parallel resonant condition with C_p and L_s at high power conditions. Once achieved the diode and choke assembly is positioned to a point where insertion loss is minimized under low power conditions. To enable both high isolation and low insertion loss to be secured under high and low power conditions respectively, a sufficiently low capacitance diode must be used for a single physical placement to be effective. Normally this capacitance value must be under 1.0$\mu\mu$f.

Next to the sectional view of the single element limiter in Figure (8), a typical low level insertion loss curve is plotted. This curve shows a resonance condition to exist and typical loaded Q values that can be expected are in the order of 7.0. Therefore, to widen bandwidth, two identical structures may be employed as shown in the lower portion of Figure (8). By control of spacing, ϕ, a much broader bandwidth may be achieved as shown. Scales for both plots in Figure (8) are assumed to be the same.

Performance characteristics of such a two-element configuration are shown in Figure (9). In the insertion loss plot, a bandwidth of 600 MC is achieved with 1.2 DB insertion loss set as the maximum limit. For this particular case, this represents a bandwidth of 6.5%. Diodes used were a PIN in the first high

power stage followed by a varactor. Both were contained in pill type packages and had measured zero bias capacitance values of approximately 0.3μμf. Breakdown voltage values were 300 V and 6 V respectively. As in the S-band case, an external diode was used to enhance limiting action of the PIN.

In Figure (8) both spike and flat leakage over the frequency band are plotted for an incident peak power level of 500 watts. Tests of a similar nature were made on other units up to power levels of 750 watts peak but resulted in the destruction of several diodes. Therefore assuming 500 watts peak to be the present capability, a spike leakage of 1.0 erg and flat level of 100 mw max can be obtained. Though this would be sufficient for protecting rugged X-band crystal diodes, a reduction of at least 3 DB would be desirable for insurance. During tests, the spike width was measured and found to approximate a rectangular pulse of 20 to 30 nanoseconds duration.

CONCLUSIONS

With respect to work performed as of date, a 1000 and 500 watt peak power capability has been achieved at S- and X-bands respectively. Though the S-band power performance was secured previous to this contract, an ATR analysis had never been done before. This mode of operation offers interesting possibilities due to its theoretically higher power handling capability.

As for S-band operation, it appears too early to draw any important conclusion other than a partial verification of the limiter equivalent circuit. As for X-band, excellent progress has been made and a 1 KW peak power capability can be achieved as of date by paralleling two units with hybrids. It is reasonable to expect that this capability will at least be doubled in the near future resulting in partial achievement of contract target specifications. Extending the present 6.5% bandwidth to 10% also appears reasonable.

PART II

PROGRAM FOR NEXT INTERVAL

Because of the highly successful results achieved at X-band to date, work during the next period will be concentrated on raising S-band peak power capability. However, some effort will be conducted on the X-band region with respect to bandwidth. As new and improved PN-junction limiter diode types become available, they will be subjected to high power tests in both areas.

Also planned for the next period is a further analysis of existing modes of operation and investigation of new types. In addition, a theoretical analysis on diode peak power handling capability will be started if time permits.

LIST OF ILLUSTRATIONS

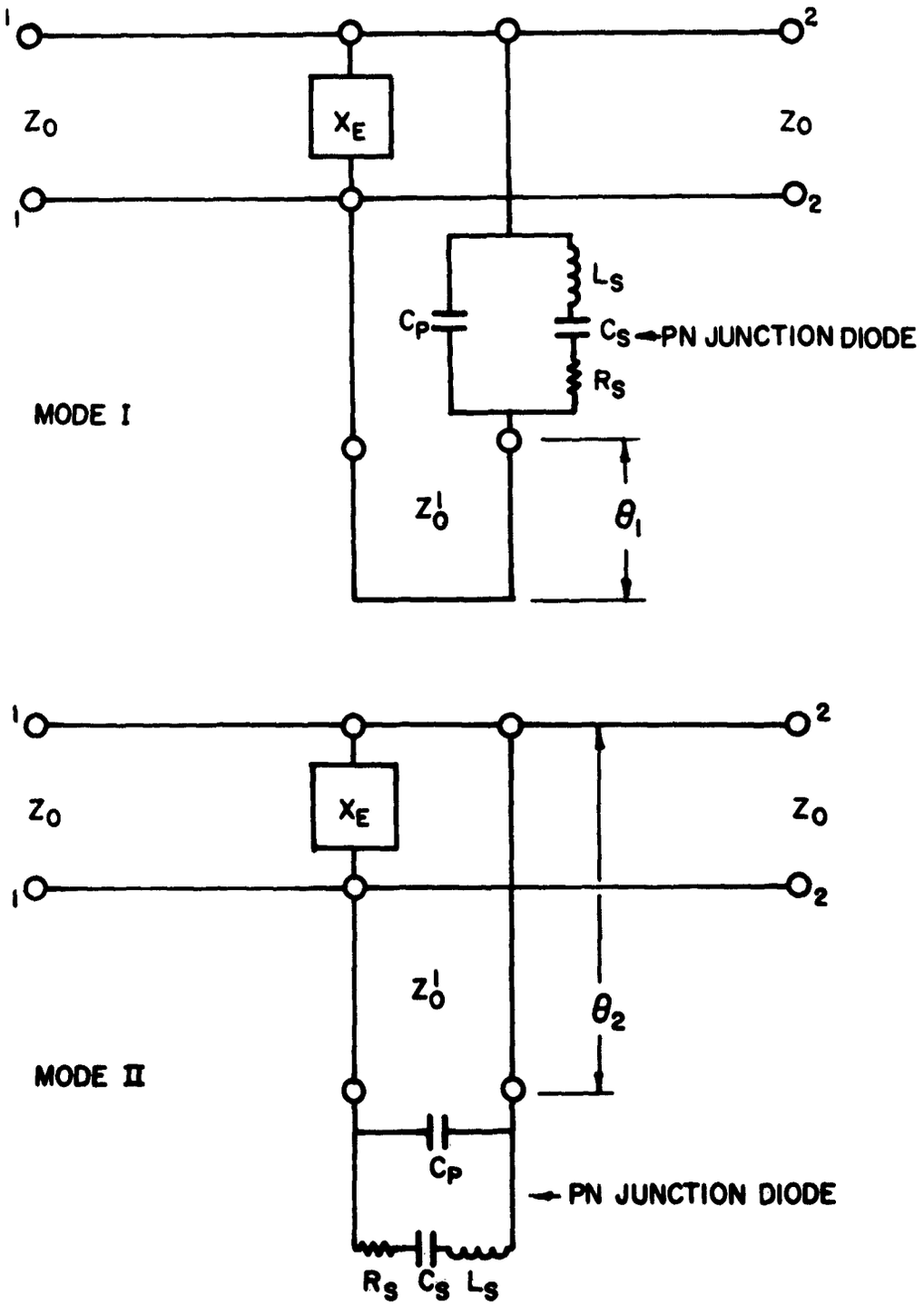

FIGURE I
EQUIVALENT CIRCUITS OF SHUNT TRANSMISSION PN JUNCTION LIMITERS, MODES I AND II.

SHUNT TRANSMISSION MODE LIMITER LOSS EQUATIONS

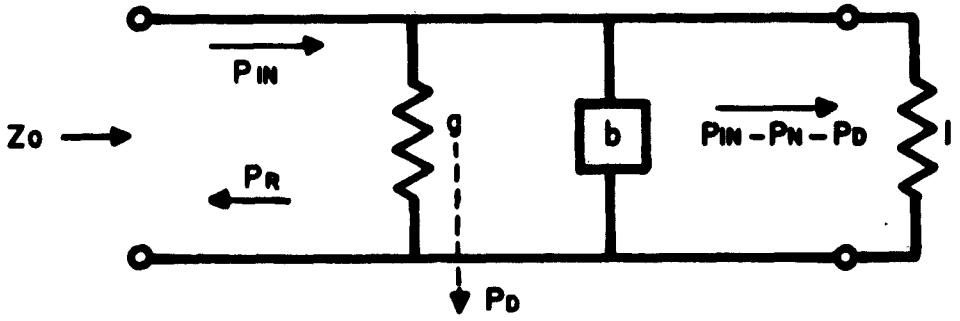

$$IL = \text{INSERTION LOSS} = \frac{P_{IN}}{P_O} = \frac{P_{IN}}{P_{IN} - P_D - P_R}$$

$$= 1 + \frac{g^2 + b^2 + 4g}{4}$$

$$RL = \text{REFLECTION LOSS} = \frac{P_{IN}}{P_{IN} - P_R}$$

$$= 1 + \frac{g^2 + b^2}{4(1+g)}$$

$$DL = \text{DISSIPATION LOSS} = \frac{P_{IN}}{P_{IN} - P_D}$$

$$= 1 + \frac{4g}{g^2 + b^2 + 4}$$

$$\frac{1}{IL} + 1 = \frac{1}{RL} + \frac{1}{DL}$$

WHERE P_{IN} IS THE INPUT POWER

" P_O IS THE OUTPUT POWER

" P_R IS THE REFLECTED POWER

" P_D IS THE DISSIPATED POWER

" g IS THE NORMALIZED SHUNT CONDUCTANCE

" b IS THE NORMALIZED SHUNT SUSCEPTANCE

FIGURE 2

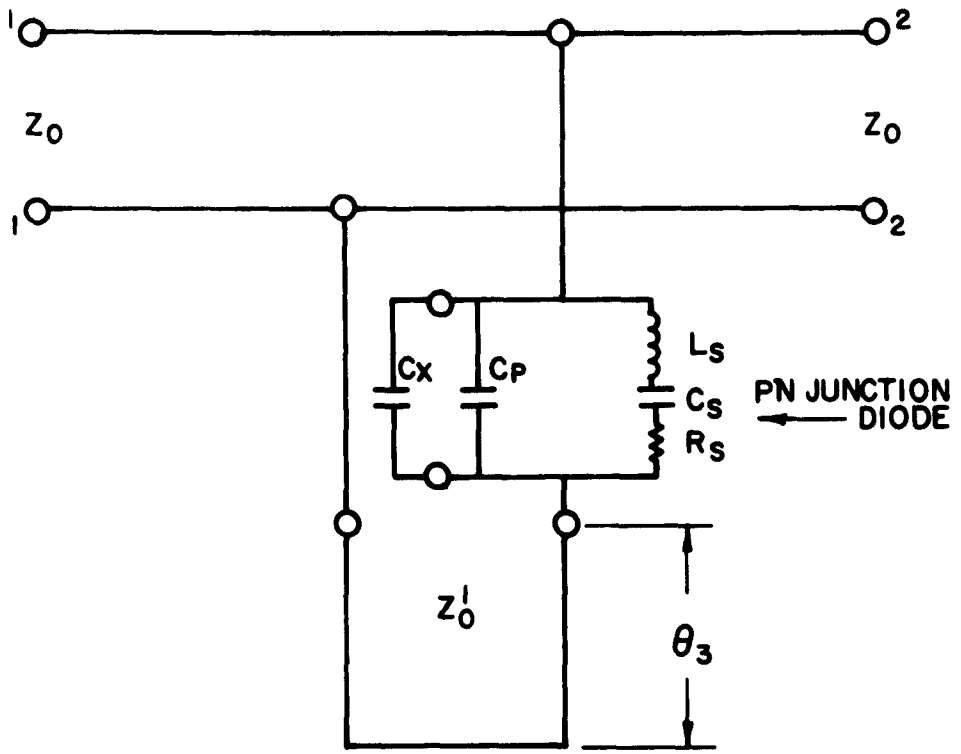

FIGURE 3
EQUIVALENT CIRCUIT OF A SHUNT REFLECTION MODE PN JUNCTION LIMITER.

SHUNT REFLECTION MODE LIMITER LOSS EQUATIONS

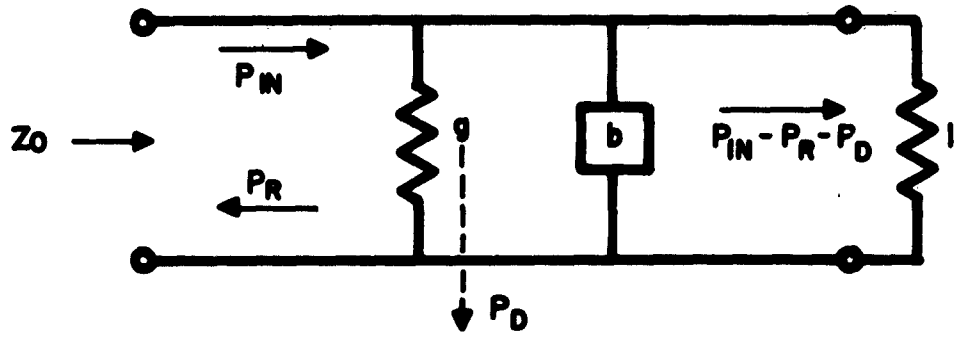

$$IL = \text{INSERTION LOSS} = \frac{P_{IN}}{P_R} = 1 + \frac{4(1+g)}{g^2 + b^2}$$

$$DL = \text{DISSIPATION LOSS} = \frac{P_{IN}}{P_{IN} - P_D} = 1 + \frac{4g}{g^2 + b^2 + 4}$$

$$TL = \text{TRANSMISSION LOSS} = \frac{P_{IN}}{P_{IN} - P_R - P_D} = 1 + \frac{g^2 + b^2 + 4g}{4}$$

$$\frac{1}{IL} + \frac{1}{TL} = \frac{1}{DL}$$

WHERE P_{IN} IS THE INPUT POWER

" P_O IS THE OUTPUT POWER

" P_R IS THE REFLECTED POWER

" P_D IS THE DISSIPATED POWER

" g IS THE NORMALIZED SHUNT CONDUCTANCE

" b IS THE NORMALIZED SHUNT SUSCEPTANCE

FIGURE 4

SHUNT TRANSMISSION MODE 2

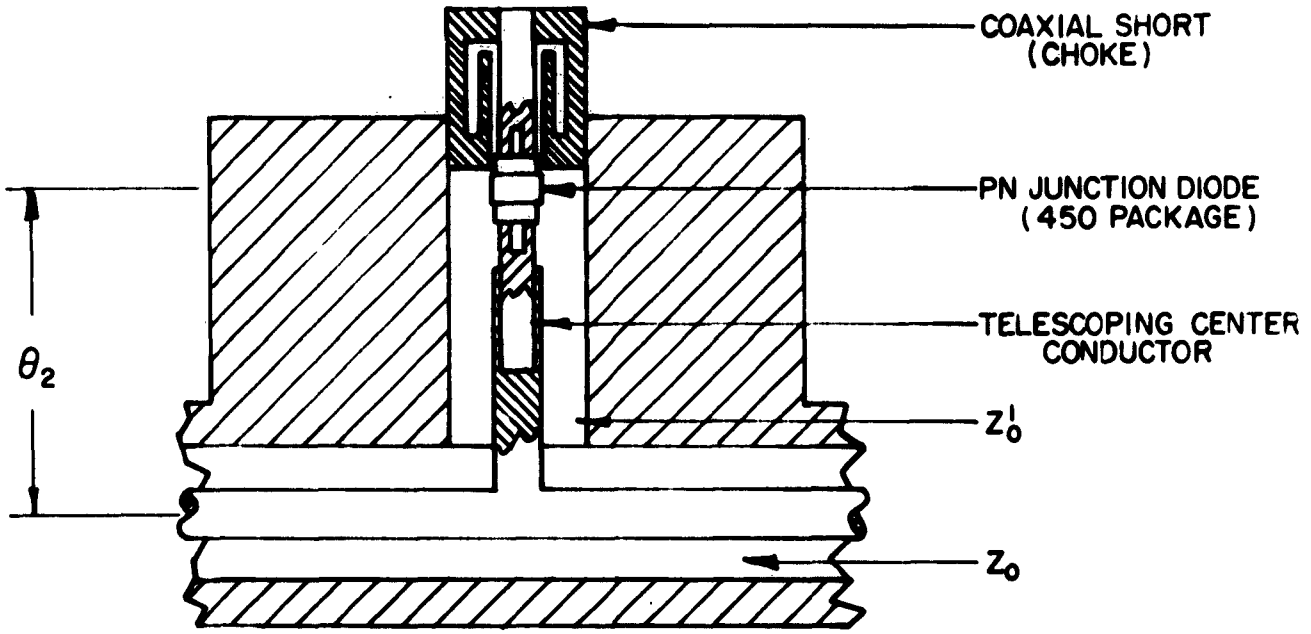

SHUNT REFLECTION MODE

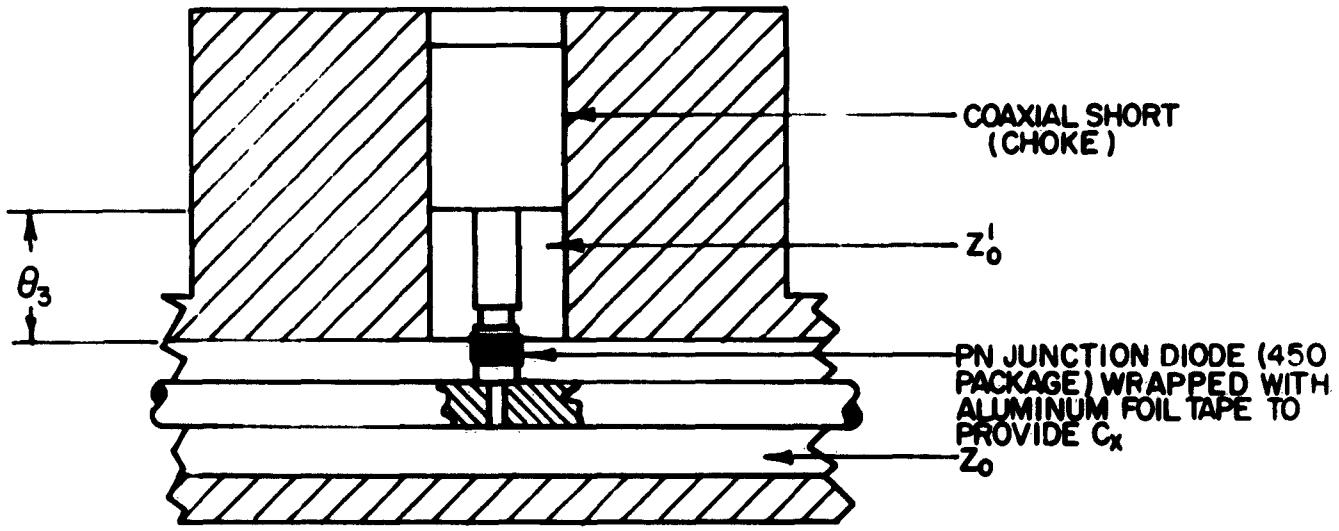

FIGURE 5
SEVERAL S BAND COAXIAL LIMITER CONFIGURATIONS

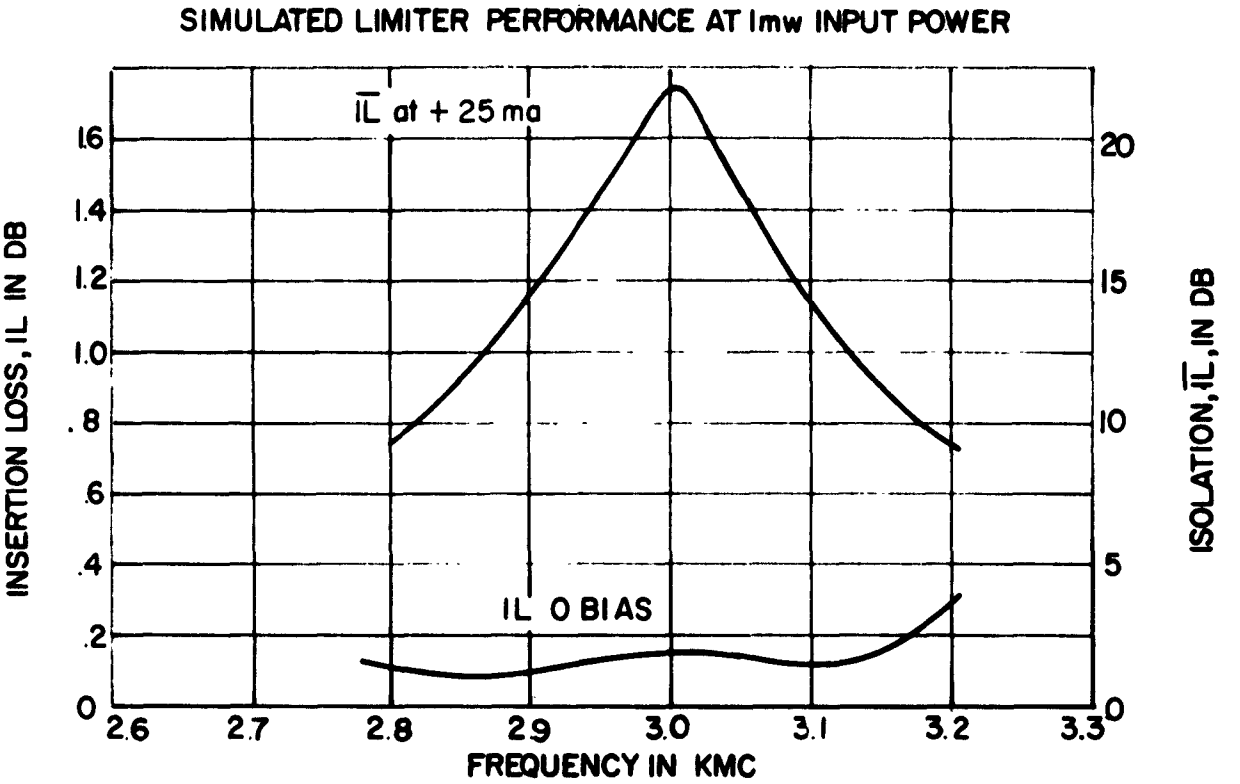

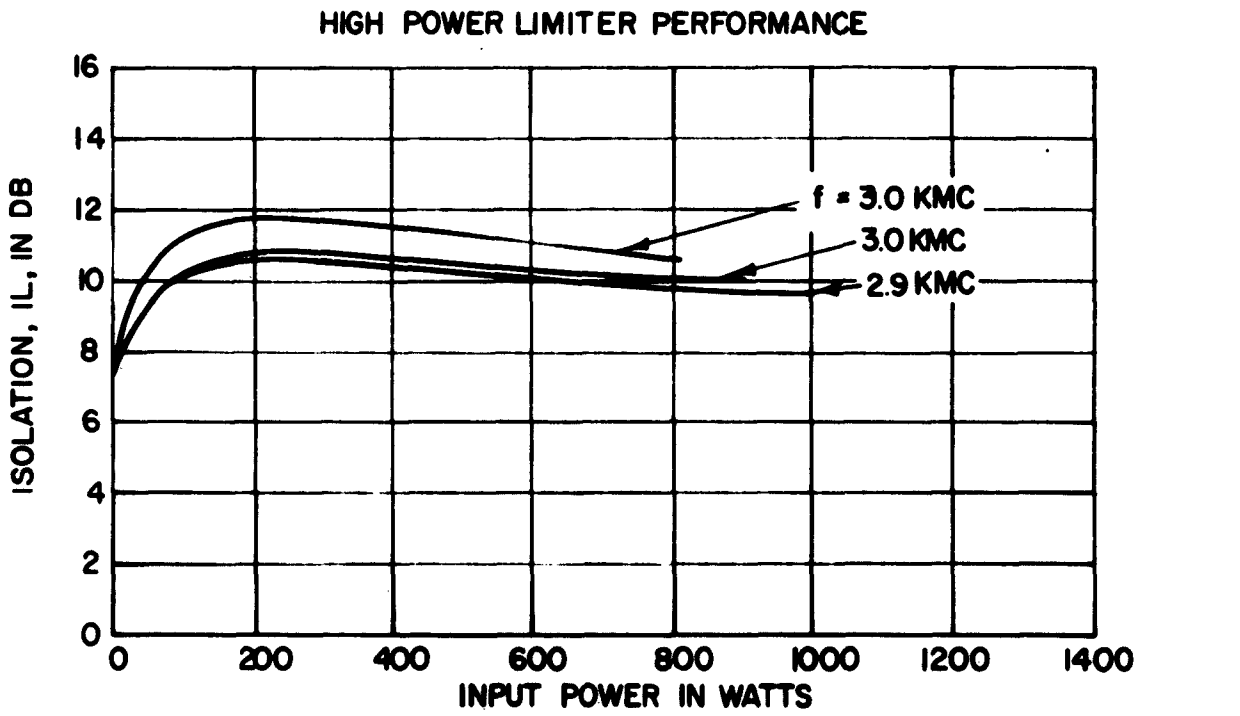

FIGURE 6
PERFORMANCE CHARACTERISTICS OF A SHUNT TRANSMISSION MODE 2 PN JUNCTION DIODE LIMITER ($Z_0 = Z_0' = 50\Omega$).

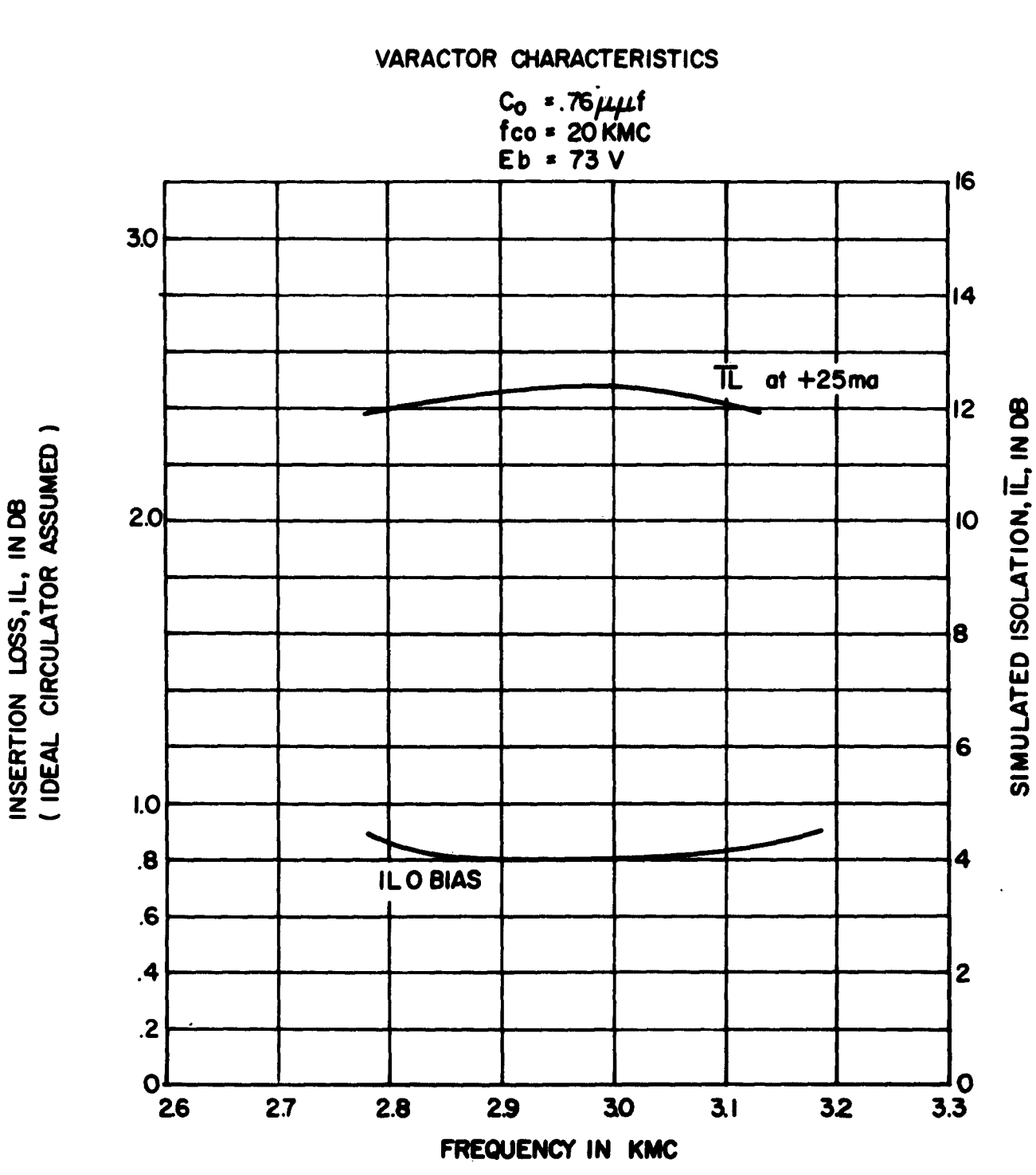

FIGURE 7

LOW POWER PERFORMANCE CHARACTERISTICS OF A SHUNT REFLECTION MODE PN JUNCTION DIODE LIMITER ($Z_g = Z_0 = 50\Omega$)

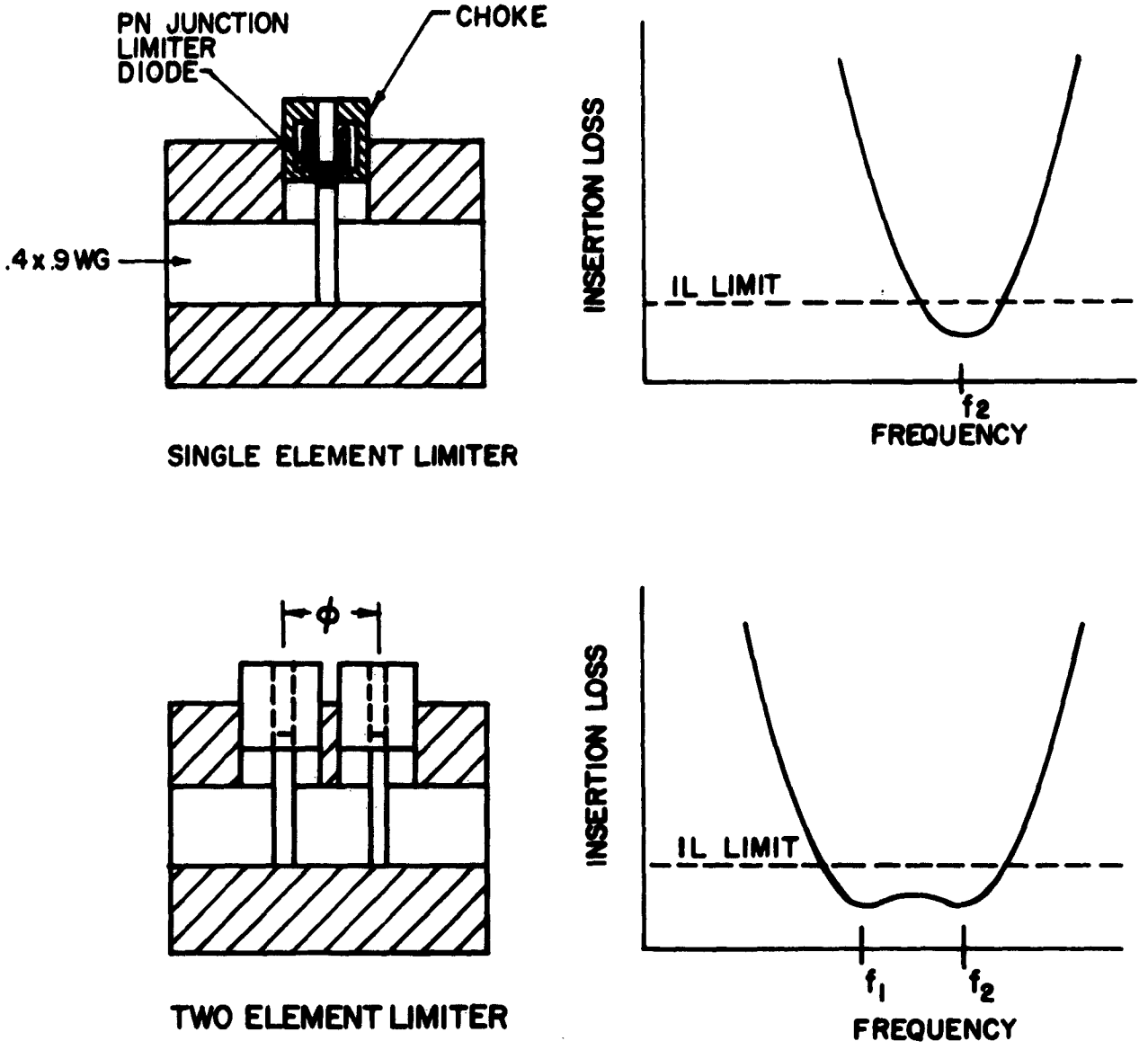

FIGURE 8

PICTORIAL COMPARISON OF A SINGLE AND TWO ELEMENT X BAND PN-JUNCTION DIODE LIMITER WITH RESPECT TO CONSTRUCTION AND LOW LEVEL PERFORMANCE.

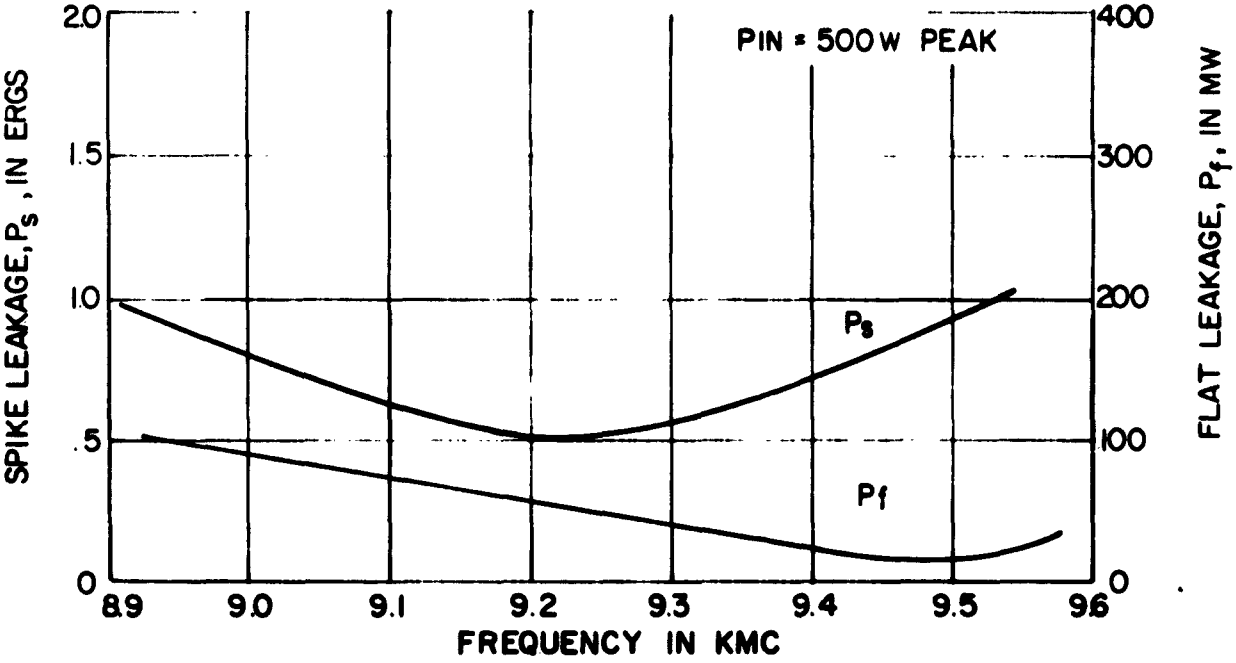

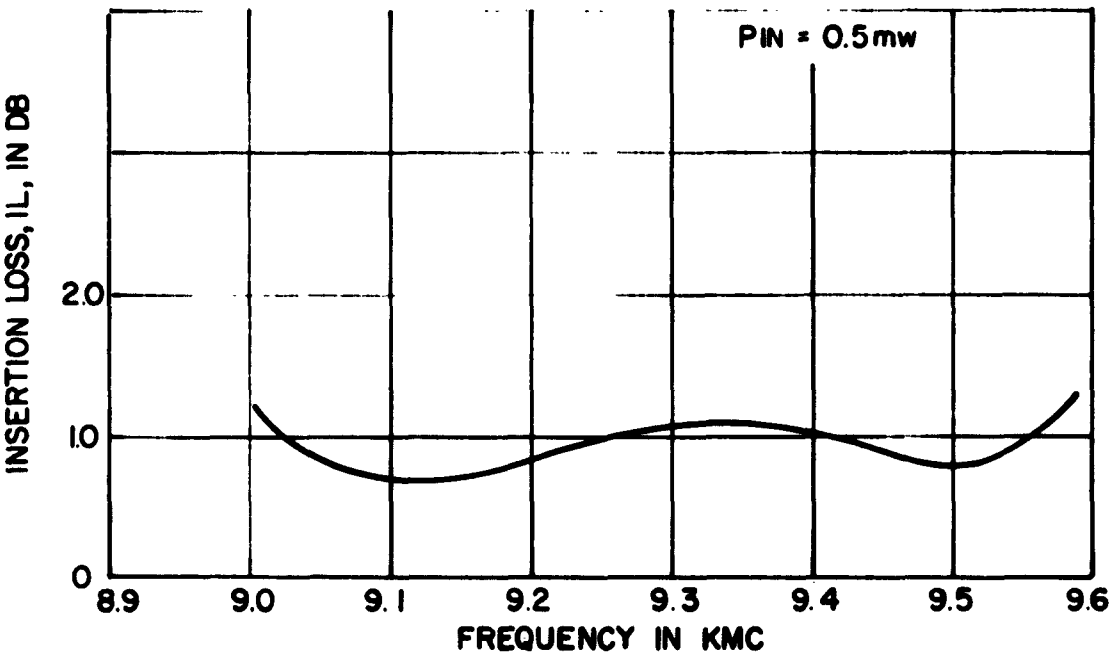

FIGURE 9
X BAND TWO ELEMENT SHUNT TRANSMISSION, MODE 2, PN JUNCTION LIMITER PERFORMANCE CHARACTERISTICS AT LOW AND HIGH POWER LEVELS.

AD_____ Accession No._____

MICROWAVE ASSOCIATES, INC.
BURLINGTON, MASSACHUSETTS

REFINEMENT PROGRAM ON ELECTRON TUBE S-BAND TR EST-27

R. Damon, R. Tenenholtz, E. Vitagliano

Final Report, 29 April 1960 to 31 August 1962

56 pp - Illus. - Graphs, Signal Corps Contract No. DA-36-039-SC-85316
Unclassified Report

Phase I - Final design, fabrication and tests have been performed on nine units of the improved mechanically-tunable EST-27 S-band TR tube. A discussion of techniques employed in construction is presented along with a comparison of performance and required specifications.

Phase II - Final design, fabrication and tests have been performed on two electronically tunable units operationally equivalent to the mechanically tunable version in Phase I. A tunable YIG filter is used in conjunction with a conventional broadband TR tube. A discussion is presented on the problems encountered, and methods employed in their solution. Performance data on the TR section, YIG filter and combination of both are given. A comparison is made with respect to required specifications.

UNCLASSIFIED

1. Refinement Program on Electron Tube S-Band TR EST-27

2. Contract No. DA-36-039-SC-85316

AD_____ Accession No._____

MICROWAVE ASSOCIATES, INC.
BURLINGTON, MASSACHUSETTS

REFINEMENT PROGRAM ON ELECTRON TUBE S-BAND TR EST-27

R. Damon, R. Tenenholtz, E. Vitagliano

Final Report, 29 April 1960 to 31 August 1962

56 pp - Illus. - Graphs, Signal Corps Contract No. DA-36-039-SC-85316
Unclassified Report

Phase I - Final design, fabrication and tests have been performed on nine units of the improved mechanically-tunable EST-27 S-band TR tube. A discussion of techniques employed in construction is presented along with a comparison of performance and required specifications.

Phase II - Final design, fabrication and tests have been performed on two electronically tunable units operationally equivalent to the mechanically tunable version in Phase I. A tunable YIG filter is used in conjunction with a conventional broadband TR tube. A discussion is presented on the problems encountered, and methods employed in their solution. Performance data on the TR section, YIG filter and combination of both are given. A comparison is made with respect to required specifications.

UNCLASSIFIED

1. Refinement Program on Electron Tube S-Band TR EST-27

2. Contract No. DA-36-039-SC-85316

AD_____ Accession No._____

MICROWAVE ASSOCIATES, INC.
BURLINGTON, MASSACHUSETTS

REFINEMENT PROGRAM ON ELECTRON TUBE S-BAND TR EST-27

R. Damon, R. Tenenholtz, E. Vitagliano

Final Report, 29 April 1960 to 31 August 1962

56 pp - Illus. - Graphs, Signal Corps Contract No. DA-36-039-SC-85316
Unclassified Report

Phase I - Final design, fabrication and tests have been performed on nine units of the improved mechanically-tunable EST-27 S-band TR tube. A discussion of techniques employed in construction is presented along with a comparison of performance and required specifications.

Phase II - Final design, fabrication and tests have been performed on two electronically tunable units operationally equivalent to the mechanically tunable version in Phase I. A tunable YIG filter is used in conjunction with a conventional broadband TR tube. A discussion is presented on the problems encountered, and methods employed in their solution. Performance data on the TR section, YIG filter and combination of both are given. A comparison is made with respect to required specifications.

UNCLASSIFIED

1. Refinement Program on Electron Tube S-Band TR EST-27

2. Contract No. DA-36-039-SC-85316

AD_____ Accession No._____

MICROWAVE ASSOCIATES, INC.
BURLINGTON, MASSACHUSETTS

REFINEMENT PROGRAM ON ELECTRON TUBE S-BAND TR EST-27

R. Damon, R. Tenenholtz, E. Vitagliano

Final Report, 29 April 1960 to 31 August 1962

56 pp - Illus. - Graphs, Signal Corps Contract No. DA-36-039-SC-85316
Unclassified Report

Phase I - Final design, fabrication and tests have been performed on nine units of the improved mechanically-tunable EST-27 S-band TR tube. A discussion of techniques employed in construction is presented along with a comparison of performance and required specifications.

Phase II - Final design, fabrication and tests have been performed on two electronically tunable units operationally equivalent to the mechanically tunable version in Phase I. A tunable YIG filter is used in conjunction with a conventional broadband TR tube. A discussion is presented on the problems encountered, and methods employed in their solution. Performance data on the TR section, YIG filter and combination of both are given. A comparison is made with respect to required specifications.

UNCLASSIFIED

1. Refinement Program on Electron Tube S-Band TR EST-27

2. Contract No. DA-36-039-SC-85316